SiC nanowire vapor–liquid–solid growth using vapor-phase catalyst delivery

Rooban Venkatesh K.G. Thirumalai and Bharat Krishnan
Department of Electrical and Computer Engineering, Mississippi State University, Mississippi State, Starkville, Mississippi 39762

Albert V. Davydov
Material Measurement Laboratory, National Institute of Standards and Technology, Gaithersburg, Maryland 20899

J. Neil Merrett
Air Force Research Laboratory, Wright-Patterson Air Force Base, Dayton, Ohio 45433

Yaroslav Koshka[a)]
Department of Electrical and Computer Engineering, Mississippi State University, Mississippi State, Starkville, Mississippi 39762

(Received 30 March 2012; accepted 14 May 2012)

A method of growing SiC nanowires (NWs) on 4H–SiC surfaces by in situ vapor-phase catalyst delivery was developed as an alternative to the ex situ deposition of the metal catalyst on the targeted surfaces before the NW chemical vapor deposition (CVD) growth. In the proposed method, sublimation of the catalyst from a metal source placed in the hot zone of the CVD reactor, followed by condensation of the catalyst-rich vapor on bare substrate surface was used to form the catalyst nanoparticles required for the vapor–liquid–solid (VLS) growth of SiC NWs. The NW density was found to gradually decrease downstream from the catalyst source and was influenced by both the gas flow rate and by the catalyst diffusion through the boundary layer above the catalyst source. Formation of poly-Si islands at too low value of the C/Si ratio created preferential nucleation centers for misaligned SiC NWs and NW bushes. The flexibility of controlling the nanoparticle density made this technique suitable for NW growth on horizontal surfaces as well as on patterned SiC substrates, including the vertical sidewalls of SiC mesas.

I. INTRODUCTION

SiC nanowires (NWs) are attractive because of this semiconductor's wide band gap, high electrical breakdown strength, and radiation resistance. SiC mechanical strength and thermal conductivity[1] are one of the best of all semiconductors available. High chemical stability and biocompatibility[2–4] make SiC NWs very promising for biomedical, sensor, and other applications in harsh environments.[2,5,6] Among many SiC NW growth methods, the chemical vapor deposition (CVD) appears to be one of the most promising to ensure adequate control of the NW growth morphology and direction, SiC polytype, crystal quality, etc.[7–9] Various substrates have been used for SiC NW synthesis, including SiO_2,[9–11] graphite,[12–15] poly-SiC,[7] and single-crystalline 4H and 6H,[16–18] typically producing NWs of 3C–SiC polytype. More rare SiC NW polytypes include 6H,[7,12,13] 2H,[7,10] and 15R.[7,15] Only a few studies have reported traces of the 4H polytype.[15,19]

It remains difficult to fabricate NWs of single polytype that replicates the one of the substrate. However, some cases of homoepitaxial and heteroepitaxial growth on SiC substrates have been reported.[16,18] In our previous work,[18] six preferential NW orientations with respect to the substrate have been obtained when growing NWs on the (0001) substrate surface by vapor–liquid–solid (VLS) method.

Achieving sufficiently rare density of NW on a substrate by using the seeded catalyst method remains a challenge, making it difficult to investigate the growth directions of individual wires in a highly packed "bundle" of interlaced NWs. Furthermore, growth on other substrate surfaces, e.g., on the vertical sidewalls of SiC mesas may be desirable to explore alternative crystallographic orientations of the NW growth axis or to form specific NW structures suitable for device or test structure fabrication. Alternatives to the seeded catalyst method when growing on patterned substrates may be desirable depending on particular requirements to the NW density, thickness, etc.

So-called floating catalyst method for growing carbon nanotubes (CNTs) was developed to provide in situ catalyst delivery.[20] The floating catalyst CVD of CNT utilized Fe catalyst supplied by vaporization of ferrocene

[a)]Address all correspondence to this author.
e-mail: ykoshka@ece.msstate.edu
This author was an editor of this focus issue during the review and decision stage. For the *JMR policy* on review and publication of manuscripts authored by editors, please refer to http://www.mrs.org/jmr-editor-manuscripts/
DOI: 10.1557/jmr.2012.208

 © Materials Research Society 2012

https://doi.org/10.1557/jmr.2012.208 Published online by Cambridge University Press

leading to formation of gaseous iron species followed by precipitation of iron clusters.[21] Alternatively, $FeCl_2$ powder was used as the catalyst source for the vapor-phase catalyst delivery for the CNT growth.[22] Vapor-phase transfer of different metals has been also utilized to form metal catalyst nanodots.[23] While the size of such nanoclusters and the temperature of their transfer/formation appear to be suitable for enabling VLS growth mode for a number of semiconductor materials, techniques similar to the floating catalyst method have not been extensively applied for the growth of semiconductor NWs.

In this work, a technique utilizing vapor-phase delivery of a metal catalyst to the substrate surface for epitaxial growth of SiC NWs has been investigated.

II. EXPERIMENTAL DETAILS

A typical hot-wall CVD reactor designed for epitaxial SiC film growth was utilized for NW growth in this work. The growth was conducted on at 1150 °C and 150 Torr using H_2 carrier gas, and $SiCl_4$ and CH_3Cl as silicon and carbon sources, respectively.[18] Commercial 8° off-axis n-type 4H–SiC (0001) substrates were used in all the experiments. In one of the experiment, the NW growth was conducted on the 4H–SiC substrate surface covered with a polycrystalline SiC layer. To investigate the potential of vapor-phase catalyst delivery for growth on patterned surfaces, 4H–SiC mesas of varying dimensions were formed by reactive ion etching (RIE) with a 9:1 ratio of SF_6/O_2 at 70 mTorr using Ni as an etch mask (Fig. 1). Resulting mesas were between 10 and 17 μm tall. A 4-h dry oxidation was performed at 1100 °C and then removed in a buffered HF solution. Etching of the mesa surfaces in H_2 ambient at 1500 °C was conducted on selected samples before using them for the NW growth. The purpose of the etching was to reduce surface roughness, which could serve as heterogeneous nucleation sites for the NW growth. Hydrogen etching duration was varied between 15 and 20 min at hydrogen flow of 10 L/min.

Either a sacrificial SiC piece coated with a NiSi layer or a SiC growth substrate with selectively patterned NiSi regions (silicon–nickel alloy of 1:1 composition) was used as a catalyst supplier for the vapor-phase delivery. The 0.2-um-thick NiSi layers were deposited by sputtering in Ar from a NiSi target. The patterned NiSi layers were formed by using a conventional liftoff photolithography technique. Also, NW growth runs were performed using 0.6–5-nm-thick layers of Ni either blanket or selectively deposited on the substrates as an alternative catalyst source. In selected experiments, 20-nm-diameter Ni nanoparticles were spin-coated from the isopropanol suspension onto the substrate surface to be used as the catalyst source.

The NWs were characterized by Nomarski optical microscopy, scanning electron microscopy (SEM), and x-ray diffraction (XRD).

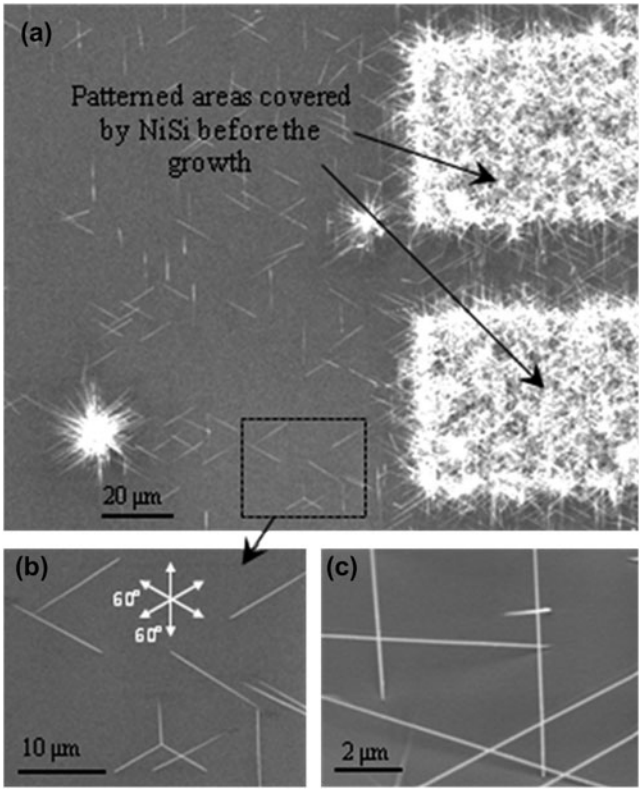


FIG. 1. (a) A SEM top view of SiC NWs growing on the (0001) surface of a 4H–SiC substrate in the regions covered with NiSi catalyst as well as on the not covered surface by the vapor-phase catalyst delivery mechanism. (b) and (c) show magnified top and tilted (20° tilt) views showing substrate-dependent orientations[18] of the NWs growing by the vapor-phase catalyst delivery mechanism. In addition, some bushes of misaligned NWs can be observed in (a).

III. RESULTS AND DISCUSSION

As expected, SiC NW growth was observed at the substrate locations covered with the metal catalyst (Fig. 1). As was reported earlier, the growth proceeded through the VLS mechanism.[18] This happens due to dewetting of the thin metal layer into discrete nanosized islands at elevated temperature, which then serve as the nucleation sites for catalytic VLS growth of NWs. In addition to that, NWs, even though with much lower density, were found in the regions on the substrate that were not originally covered with the catalyst (Fig. 1). Apparently, this secondary growth proceeded due to a vapor transfer of the catalyst from the source areas into those regions of the substrate not covered with a catalyst. Energy-dispersive x-ray spectroscopy (EDS) analysis confirmed the presence of Ni in the metal droplets at the tip of the NWs. The chemical composition of the metal droplet was similar to that measured from the metal droplets in NWs produced by the regular seeded catalyst method.[18]

Closer look at these areas [Figs. 1(b) and 1(c)] revealed that the NWs grow epitaxially with their axes aligned along one of six directions with respect to the substrate.[18] XRD and EDS results were very similar to those reported

https://doi.org/10.1557/jmr.2012.208 Published online by Cambridge University Press

for NWs produced by the regular seeded catalyst method in Ref. 18 and confirmed that only SiC NWs were formed. It should be mentioned that achieving such low NW density was very difficult when using the regular seeded catalyst method. Investigation of the polytype and the crystalline structure of these NWs is beyond the scope of this paper and is reported elsewhere.[24]

A similar result has been achieved when a small seed sample coated with a metal catalyst layer was placed upstream from the growth substrate. NWs of varying density were observed across the surface of the growth substrate even when the substrate was positioned at a significant distance (e.g., more than 10 mm) away from the catalyst source. Both the in situ catalyst deposition and the degree of the precursor supersaturation inside the catalyst during the VLS growth should depend on the temperature. Therefore, variations of the thermal conditions between the edges of the small substrates and their middle regions were expected to introduce additional nonhomogeneity of the NW density. To eliminate the contribution of this nonhomogeneity when investigating the two-dimensional distribution of the NW pattern with respect to the catalyst source, the NW density was analyzed after growing NWs across the entire 2-inch SiC substrate that is normally used as the wafer carrier. Figure 2(a) shows the 2-inch 4H–SiC wafer carrier covered with dense NWs grown due to the vapor-phase transfer of the catalyst from the catalyst source. The milky (i.e., the white) regions correspond to the higher NW density [as revealed by the magnified image in Fig. 2(b)]. The dark square region in the middle of the wafer carrier shows the position of the catalyst source (a piece of a substrate covered with a layer of NiSi). It should be noted that the overall NW density on the surface of the wafer carrier is much higher than that in Fig. 1. This is due to the fact that the surface of the wafer carrier had a polycrystalline layer of SiC before the NW growth, which created much higher density of preferential surface cites for the in situ catalyst deposition and NW growth. However, this surface was convenient for investigating the NW density variation with respect to the catalyst source.

The region of high NW density was found to be significantly extended along the gas flow direction downstream from the catalyst source [Fig. 2(a)]. This indicated that the gas flow (i.e., the forced convection) is responsible for transferring the metal catalyst inside the hot zone over more than a few centimeters from the source. However, high NW density was also found upstream from the source [Fig. 2(a)]. Since it is known that a laminar flow is established inside the hot zone of this reactor, only gas-phase diffusion through the stagnant layer above the surface of the wafer carrier (i.e., the boundary layer) could be responsible for the catalyst transfer in the upstream direction from the source. Naturally, the catalyst-carrying gas-phase species, which diffuse upward through the stagnant layer and reach the main gas stream, get picked up by the gas flow and transported over significant distances before aggregating into metal clusters at the growth surface contributing to the NW growth by the VLS mechanism.

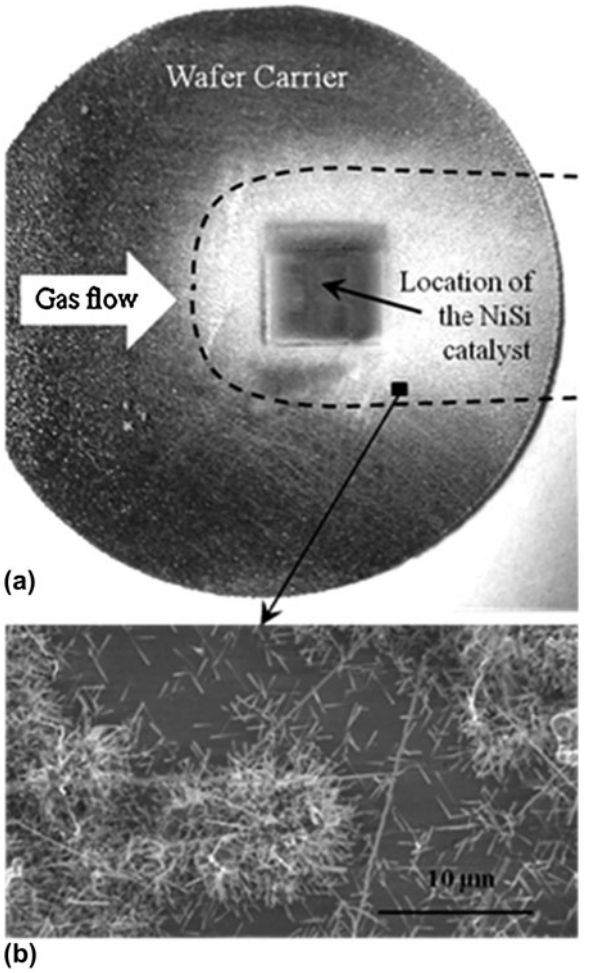


FIG. 2. (a) A photograph of the wafer carrier after NW growth. One can see the location of a 1 × 1 cm substrate covered with NiSi that was used as the catalyst source. The dotted line shows the approximate boundary of the NW region formed by the vapor-phase catalyst delivery—the white area surrounding the location of the catalyst. Both the diffusion through the boundary layer and the gas flow direction influence the macroscopic NW distribution. (b) A SEM image of the NWs growing on the wafer carrier due to the vapor-phase catalyst delivery mechanism.

While a systematic comparison of different metal catalysts was outside of the scope of this study, qualitatively, similar results were obtained when using Ni metal layer as a source of the catalyst for the vapor-phase delivery. It should be noted that even if the optimal temperature range for the vaporization and transfer of the catalyst is different for the Ni and NiSi sources, the temperature in the hot zone is even more crucial for the gas-phase and surface reactions of the NW growth precursors and the VLS growth mechanism. This makes it difficult

https://doi.org/10.1557/jmr.2012.208 Published online by Cambridge University Press

to decouple the temperature dependence of the vapor-phase catalyst delivery from that of the chemical reactions involved in the NW growth. Furthermore, the well-known process of silicidation of thin Ni layers on the top of SiC surface is likely to further reduce the differences between the Ni and NiSi sources.

Ni nanoparticles of 20 nm diameter deposited on the catalyst source substrate by the spin-on deposition technique were also used to study vapor-phase catalyst delivery. Both the seeded catalyst NW growth on the samples serving as the catalyst source and the growth by the vapor-phase catalyst delivery on the bare substrate were found to be qualitatively similar to that using the blanket deposited Ni. However, the control of the NW density is yet to be optimized, which is complicated by a poor control of the density of the Ni nanoparticles following the spin-on deposition.

Finally, some localized NW growth was observed even when no catalyst source was used in a particular run due to residual contamination of the hot zone with a catalyst from the previous runs. This "catalyst memory effect" usually persisted for a few growth runs before being gradually eliminated by etching the hot zone with hydrogen carrier gas at elevated temperatures (e.g., above 1500 °C). No self-nucleation of NWs took place in the process described in this work.

A wide range of less than favorable growth conditions outside of the optimized process window resulted in either formation of dense NWs over the entire surface [e.g., similar to Fig. 2(b)] or formation of bushes composed of randomly oriented NWs that do not follow the previously reported epitaxial growth pattern.[18] The density of the bushes was found to vary along the gas flow direction and was often increasing downstream (i.e., away from the catalyst source) [Figs. 3(a) and 3(b)]. This suggested that nucleation of dense NWs or NW bushes may be influenced by factors other than the catalyst delivery. To investigate the bushes nucleation mechanism, a supply of the metal catalyst was significantly reduced to suppress the NW growth and reveal possible nucleation centers that are otherwise hidden under the bushes. Notably, formation of polycrystalline silicon islands, similar to those from the regular catalyst-free epitaxial growth conducted at similar growth conditions,[25] was also observed in this study [see Figs. 3(c) and 3(d)]. The Si island density variation across the susceptor matched the density of the NW bushes grown at identical growth conditions with adequate supply of the metal catalyst [Figs. 3(a) and 3(b)]. An upstream location and a downstream location are shown in Fig. 3 to illustrate that the change in the density of the NW bushes from upstream to downstream correlates with the corresponding change in the size and density of the polycrystalline silicon islands.

It has been established that undesirable nucleation of the NW bushes can be reduced by increasing the C/Si ratio during the growth, which is done by adjusting the CH_3Cl and SiCl flow rates. The role of the C/Si ratio was further investigated. First, a low catalyst supply was used to avoid masking the poly-Si islands by the NW bushes. The density of the polycrystalline Si islands was found to significantly decrease with increasing the C/Si ratio (Fig. 4). No islands could be observed for the C/Si ratio above ~9. A similar trend of poly-Si island nucleation was observed during the low-temperature epitaxial growth of SiC in our previous work.[25] While the NW growth temperature of 1150 °C is lower than the 1300 °C temperature of the SiC homoepitaxial growth,[25] the surplus of Si over C (i.e., too low C/Si ratio) is expected to cause a similar solid Si phase nucleation during the NW growth. Note that we report the input (inlet) C/Si ratio, which may be significantly different from the real ("effective") C/Si ratio at the growth surface.

The influence of the C/Si ratio on the density of the NW bushes was found to match that for the poly-Si islands (Fig. 5). Relatively, big poly-Si islands that form at C/Si = 6 cause formation of NW bushes [Fig. 5(a)]. At C/Si = 9, only very small poly-Si islands should form according to Fig. 4(c), which results in growth of dense NW without formation of big bushes [Fig. 5(b)]. Finally, at C/Si = 12, no poly-Si islands form, which leads to the growth of rare individual NWs aligned along the previously reported crystallographic orientations with respect to the substrate[18] (i.e., following the epitaxial growth mode) [Fig. 5(c)]. It is logical to suggest that the rough

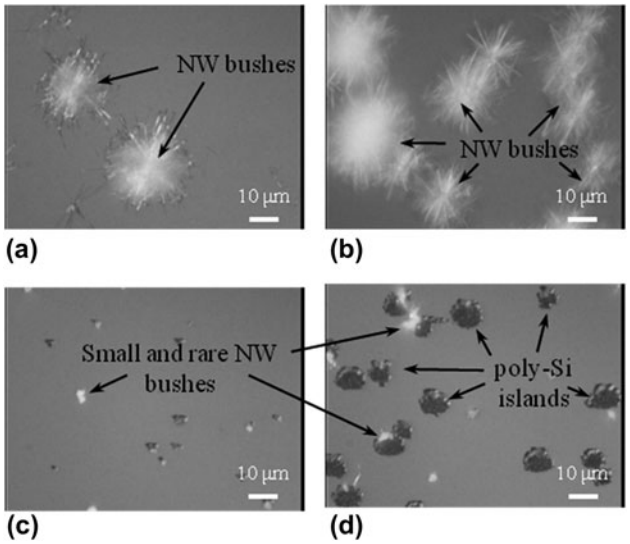


FIG. 3. Growth of NW bushes rather than individual NWs, which happens at too low value of the C/Si ratio. (a) and (b) show optical micrographs of upstream and downstream locations of a substrate, with NW bushes grown by the vapor-phase catalyst delivery mechanism. (c) and (d) are for a similar substrate, however, with significantly reduced supply of the metal catalyst. Much smaller and more rare NW bushes in (c) and (d) reveal poly-Si islands serving as nucleation centers for the NW bushes in (a) and (b).

https://doi.org/10.1557/jmr.2012.208 Published online by Cambridge University Press

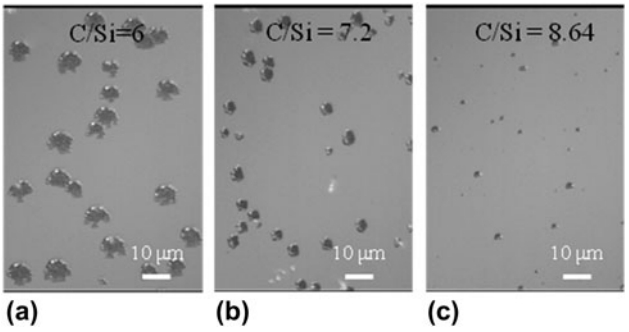


FIG. 4. Optical micrograph of poly-Si islands visible thanks to the low supply of the metal catalyst. Three different values of the C/S ratio were used: (a) C/Si = 6, (b) C/Si = 7.2, and (c) C/Si = 8.64. High enough C/Si allows entirely avoiding poly-Si island formation.

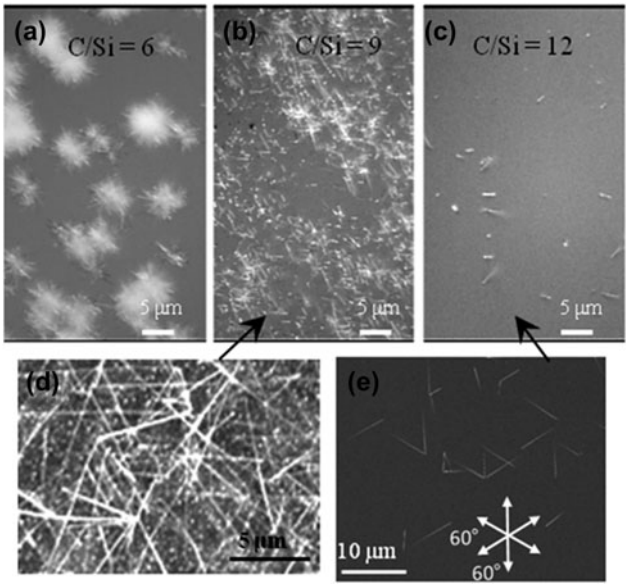


FIG. 5. Transition from bushes of NWs at C/Si = 6 (a) to dense randomly oriented NWs at C/Si = 9 (b) and to the desirable individual NWs with substrate-determined orientations at C/Si = 12 (c). (d) and (e) show SEM images for (b) and (c), respectively. This trend also correlates with the trend of poly-Si island reduction at higher C/Si ratio (Fig. 4).

surface of poly-Si islands serve as preferential sites for agglomeration of metal nanoclusters, which causes the high concentration of NWs forming the bushes.

Next, a potential of using the vapor-phase catalyst delivery technique to growing on the vertical sidewalls of SiC mesas was investigated. NWs successfully grew on all available surfaces of 4H–SiC mesas formed by RIE on the top (0001) surface of a 4H–SiC substrate (Fig. 6). Initially, very dense NWs were achieved on the vertical sidewalls [Fig. 6(a)], and their density could not be significantly reduced by merely reducing the amount of the catalyst source available for the vapor-phase catalyst delivery. It was speculated that similar to the case of the rough surface in Fig. 2 or rough surfaces of poly-Si islands

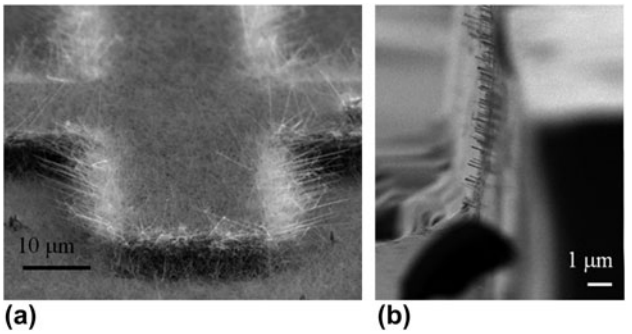


FIG. 6. Use of the vapor-phase catalyst delivery to grow on patterned surfaces: (a) dense NWs growing on the vertical mesa walls and the horizontal surfaces at high catalyst supply and significant RIE damage and (b) too low catalyst supply in combination with H2 preetching of the mesa surface causes rare spots of NW nucleation only at defects (e.g., scratches) on the vertical sidewalls.

in Figs. 4 and 5, the surface damage at the vertical sidewalls promoted heterogeneous nucleation of the metal catalyst and enhanced formation of a high-density metal clusters for VLS NW growth. To reduce the lattice damage caused by RIE, the experiment was repeated on mesas that were etched in H_2 flow at 1500 °C for 10 min before the NW growth. The NW growth was conducted without any catalyst source placed inside the hot zone, but instead, it relied exclusively on the catalyst memory effect caused by the contamination of the hot zone with the catalyst during the previous runs.

As a result of the minimized catalyst supply and significantly reduced surface roughness, the NW density was drastically reduced on most of the mesa surfaces [Fig. 6(b)]. Besides some individual rare NWs (Fig. 7), selected locations of the vertical sidewalls exhibited relatively dense NW arrays [Fig. 6(b)]. In all the cases, those arrays corresponded to a surface damage [e.g., scratches at the mesa surface as in Fig. 6(b)]. The same effect was observed when the growth was conducted on a substrates surface roughened by the presence of a poly-crystalline layer. This confirmed the conclusion that surface roughness is essential for promoting clustering of the metal catalyst at higher concentrations.

It should be noted that clear preferential growth orientations were observed for the NWs growing on the vertical sidewalls, similar to the previous study of the growth on the (0001) surface. Investigation of the growth orientation trends and the polytype and the crystalline structure of these NWs is beyond the scope of this paper and will be reported elsewhere.[24]

It is the subject of the future work to establish what exactly gas-phase species and chemical reactions are involved in vaporization of the metal catalysts and its transport to the growth surface. A relevant observation from Fig. 7 is the presence of metal droplets at the tip of the NWs, which are difficult to detect for the normally

https://doi.org/10.1557/jmr.2012.208 Published online by Cambridge University Press

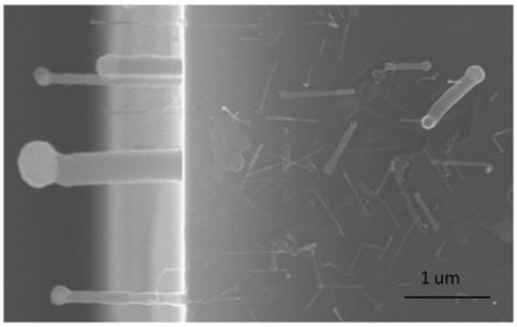


FIG. 7. A mesa samples with a few thicker NWs formed by vapor-phase catalyst delivery, which allows detecting the catalyst drop at the tip of the NWs.

thin NWs but are clearly distinguishable for more rare thick NWs. This confirmed that the vapor-phase catalyst delivery of the catalyst indeed takes place, causing the NWs grow by the VLS growth mechanism.

IV. CONCLUSIONS

Vapor-phase metal catalyst delivery mechanism has been demonstrated to be a viable technique for VLS growth of SiC NWs. The catalyst can be easily delivered to differently oriented surfaces of a complex substrate topology, as was illustrated by the growth on vertical sidewalls of SiC mesas.

While the processing temperature is expected to be an important factor for the efficiency of the metal catalyst vaporization and its delivery to the growth surface, only the range of temperatures optimal for the VLS growth itself was used in this work. Decoupling the temperature dependence of the catalyst delivery from the temperature dependence of the VLS growth may require different experimental arrangements, e.g., placement of the catalyst source more upstream from the substrate and individually controlling the temperature at this location. Since both gas-phase diffusion of the catalyst through the stagnant layer above the surface of the substrate and the catalyst transport by the main flow of the carrier gas were shown to influence the catalyst delivery to the growth surface, it offers significant flexibility for selecting the geometry of the hot zone and relative positions of the catalyst source and the growth substrate.

The roughness of the growth surface and the density of the surface defects (e.g., scratches) were found to be critical for controlling the density of the NWs, which is particularly important when well-separated individual NWs are desirable. The work is currently in progress to use the vapor-phase catalyst delivery method to study orientations of the SiC NW grown on different SiC crystallographic plains as well as to produce device structures utilizing well-aligned NWs on vertical sidewalls of SiC mesas.

REFERENCES

1. K. Zekentes and K. Rogdakis: SiC nanowires: Material and devices. *J. Phys. D: Appl. Phys.* **44**, 133001 (2011).
2. X. Li, X. Wang, R. Bondokov, J. Morris, Y.H. An, and T.S. Sudarshan: Micro/nanoscale mechanical and tribological characterization of SiC for orthopedic applications. *J. Biomed. Mater. Res. Part B* **72**, 353–361 (2005).
3. S. Santavirta, M. Takagi, L. Nordsletten, A. Anttila, R. Lappalainen, and Y.T. Konttinen: Biocompatibility of silicon carbide in colony formation test in vitro. *J. Biomater. Appl.* **118**, 89–91 (1998).
4. S.E. Saddow, C. Coletti, C.L. Frewin, N. Schettini, A. Oliveros, and M. Jarosezeski: Single-crystal silicon carbide: A biocompatible and hemocompatible semiconductor for advanced biomedical applications, in *Silicon Carbide 2010—Materials, Processing and Devices*, edited by S.E. Saddow, M. Dudley, E.K. Sanchez, and F. Zhao (Mater. Res. Soc. Symp. Proc. **1246**, Warrendale, PA, 2010) p. 193.
5. R. Yakimova, R.M. Petoral, Jr., G.R. Yazdi, C. Vahlberg, A.L. Spetz, and K. Uvdal: Surface functionalization and biomedical applications based on SiC. *J. Phys. D: Appl. Phys.* **40**, 6435–6442 (2007).
6. P.G. Neudeck, D.J. Spry, A.J. Trunek, L.J. Evans, L-Y. Chen, G.W. Hunter, and D. Androjna: Hydrogen gas sensors fabricated on atomically flat 4H-SiC webbed cantilevers. *Mater. Sci. Forum* **600–603**, 1199–1202 (2009).
7. R. Pampuch, G. Górny, and L. Stobierski: Synthesis of one-dimensional nanostructured silicon carbide by chemical vapor deposition. *Glass Phys. Chem* **31**(3), 370 (2005).
8. H.Y. Peng, X.T. Zhou, H.L. Lai, N. Wang, and S.T. Lee: Microstructure observations of silicon carbide nanorods. *J. Mater. Res.* **15**, 2020 (2000).
9. H.K. Seong, T.E. Park, S. Lee, K.R. Lee, J.K. Park, and H.J. Choi: Magnetic properties of vanadium-doped silicon carbide nanowires. *Met. Mater. Int.* **15**(1), 107 (2009).
10. Y. Yao, S.T. Lee, and F.H. Li: Direct synthesis of 2H–SiC nanowhiskers. *Chem. Phys. Lett.* **381**, 628–633 (2003).
11. H-K. Seong, H-J. Choi, S-K. Lee, J-I. Lee, and D-J. Choi: Optical and electrical transport properties in silicon carbide nanowires. *Appl. Phys. Lett.* **85**, 1256–1258 (2004).
12. H. Wang, Z. Xie, W. Yang, J. Fang, and L. An: Morphology control in the vapor-liquid-solid growth of SiC nanowires. *Cryst. Growth Des.* **8**, 3893–3896 (2008).
13. F. Gao, W. Yang, H. Wang, Y. Fan, Z. Xie, and L. An: Controlled Al-doped single-crystalline 6H-SiC nanowires. *Cryst. Growth Des.* **8**, 1461–1464 (2008).
14. R. Wu, B. Li, M. Gao, J. Chen, Q. Zhu, and Y. Pan: Tuning the morphologies of SiC nanowires via the control of growth temperature, and their photoluminescence properties. *Nanotechnology* **19**, 335602 (2008).
15. M. Bechelany, A. Brioude, D. Cornu, G. Ferro, and P. Miele: Raman spectroscopy study of individual SiC nanowires. *Adv. Funct. Mater.* **17**, 939–943 (2007).
16. H. Wang, L. Lin, W. Yang, Z. Xie, and L. An: Preferred orientation of sic nanowires induced by substrates. *J. Phys. Chem. C* **114**, 2591–2594 (2010).
17. S.G. Sundaresan, A.V. Davydov, M.D. Vaudin, and I. Levin: Growth of silicon carbide nanowires by a microwave heating-assisted physical vapor transport process using group VIII metal catalysts. *Chem. Mater.* **19**, 5531–5537 (2007).
18. B. Krishnan, R.V.K.G. Thirumalai, Y. Koshka, S. Sundaresan, I. Levin, A.V. Davydov, and J.N. Merrett: Substrate-dependent orientation and polytype control in SiC nanowires grown on 4H-SiC substrates. *Cryst. Growth Des.* **11**, 538–541 (2011).
19. H. Yoshida, H. Kohno, S. Ichikawa, T. Akita, and S. Takeda: Inner potential fluctuation in SiC nanowires with modulated interior structure. *Mater. Lett.* **61**, 3134–3137 (2007).

https://doi.org/10.1557/jmr.2012.208 Published online by Cambridge University Press

20. M. Endo and T. Koyama: Preparation of carbon fiber by vapor-phase method. Japanese Patent No. 60–027700, 1985.
21. H.M. Cheng, F. Li, G. Su, H. Pan, L.L. He, X. Sun, M.S. Dresselhaus, T. Swnts, and C. During: Large-scale and low-cost synthesis of single-walled carbon nanotubes by the catalytic pyrolysis of hydrocarbons. *Appl. Phys. Lett.* **72**, 3282–3284 (1998).
22. Y. Inoue, K. Kakihata, Y. Hirono, T. Horie, A. Ishida, and H. Mimura: One-step grown aligned bulk carbon nanotubes by chloride mediated chemical vapor deposition. *Appl. Phys. Lett.* **92**, 213113 (2008).
23. K. Wegner, B. Walker, S. Tsantilis, and S.E. Pratsinis: Design of metal nanoparticle synthesis by vapor flow condensation. *Chem. Eng. Sci.* **57**, 1753–1762 (2002).
24. R.V.K.G. Thirumalai, B. Krishnan, A.V. Davydov, J.N. Merrett, and Y. Koshka: Growth on differently-oriented sidewalls of SiC mesas as a way of achieving well-aligned SiC nanowires. *Cryst. Growth Des.* **12**, 2221–2225 (2012).
25. S. Kotamraju, B. Krishnan, G. Melnychuk, and Y. Koshka: Low-temperature homoepitaxial growth of 4H–SiC with CH3Cl and SiCl4 precursors. *J. Cryst. Growth* **312**, 645–650 (2010).

https://doi.org/10.1557/jmr.2012.208 Published online by Cambridge University Press